ADVANCED FUNCTIONAL MATERIALS
www.afm-journal.de

Materials and Wireless Microfluidic Systems for Electronics Capable of Chemical Dissolution on Demand

*Chi Hwan Lee, Jae-Woong Jeong, Yuhao Liu, Yihui Zhang, Yan Shi, Seung-Kyun Kang, Jeonghyun Kim, Jae Soon Kim, Na Yeon Lee, Bong Hoon Kim, Kyung-In Jang, Lan Yin, Min Ku Kim, Anthony Banks, Ungyu Paik, Yonggang Huang, and John A. Rogers**

Electronics that are capable of destroying themselves, on demand and in a harmless way, might provide the ultimate form of data security. This paper presents materials and device architectures for triggered destruction of conventional microelectronic systems by means of microfluidic chemical etching of the constituent materials, including silicon, silicon dioxide, and metals (e.g., aluminum). Demonstrations in an array of home-built metal-oxide-semiconductor field-effect transistors that exploit ultrathin sheets of monocrystalline silicon and in radio-frequency identification devices illustrate the utility of the approaches.

1. Introduction

Confidential data associated with military, financial, corporate, and personal systems are among the most valuable assets in modern society, justifying considerable investment in technologies for their protection. The most widely used approaches involve data encryption and access passwords, even though such software solutions have much vulnerability. Permanent destruction, at the level of the hardware (i.e., memory chips and associated electronics), represents the ultimate solution for secure data.[1–3] Here, we describe some simple concepts in wireless microfluidics and etching chemistries that enable on demand, complete dissolution of conventional microelectronic systems, with general applicability to broad classes of state-of-the-art semiconductor devices. These systems allow programmable, controlled release, and fluidic delivery of multiple highly corrosive etchants that rapidly and permanently eliminate key constituent materials, such as silicon (Si), silicon dioxide (SiO_2) and metals (e.g., Al), in memory modules, integrated circuits, and radio components. This functionality represents a triggered mode of operation for a broad, emerging area of technology known as transient electronics.[4] Several application examples demonstrate the utility of these platforms for triggered transience.

2. Results and Discussion

Figure 1a presents the structure of a wireless device for triggered transience which includes microfabricated heaters, thermally expandable polymers, fluid reservoirs, and microfluidic

Dr. C. H. Lee, Y. Liu, Dr. S.-K. Kang, Dr. B. H. Kim, Dr. K.-I. Jang, Dr. L. Yin, A. Banks, Prof. J. A. Rogers
Department of Materials Science and Engineering
Beckman Institute for Advanced Science and Technology
and Frederick Seitz Materials Research Laboratory
University of Illinois at Urbana-Champaign
Urbana, IL 61801, USA
E-mail: jrogers@illinois.edu

Prof. J.-W. Jeong
Department of Electrical
Computer, and Energy Engineering
University of Colorado
Boulder, CO 80309, USA

Dr. Y. Zhang, Y. Shi, Prof. Y. Huang
Department of Civil and Environmental Engineering,
and Mechanical Engineering
Northwestern University
Evanston, IL 60208, USA

Dr. Y. Zhang
Center for Mechanics and Materials
Tsinghua University
Beijing 100084, China

Y. Shi
State Key Laboratory of Mechanics
and Control of Mechanical Structures
Nanjing University of Aeronautics and Astronautics
Nanjing 210016, China

J. Kim, Prof. U. Paik
Department of Materials Science and Engineering
Department of Energy Engineering
Hanyang University
Seoul 133-791, Republic of Korea

J. S. Kim
Department of Chemistry
University of Illinois at Urbana-Champaign
Urbana, IL 61801, USA

N. Y. Lee
Department of Bioengineering
University of Illinois at Urbana-Champaign
Urbana, IL 61801, USA

M. K. Kim
Department of Electrical and Computer Engineering
University of Illinois at Urbana-Champaign
Urbana, IL 61801, USA

DOI: 10.1002/adfm.201403573

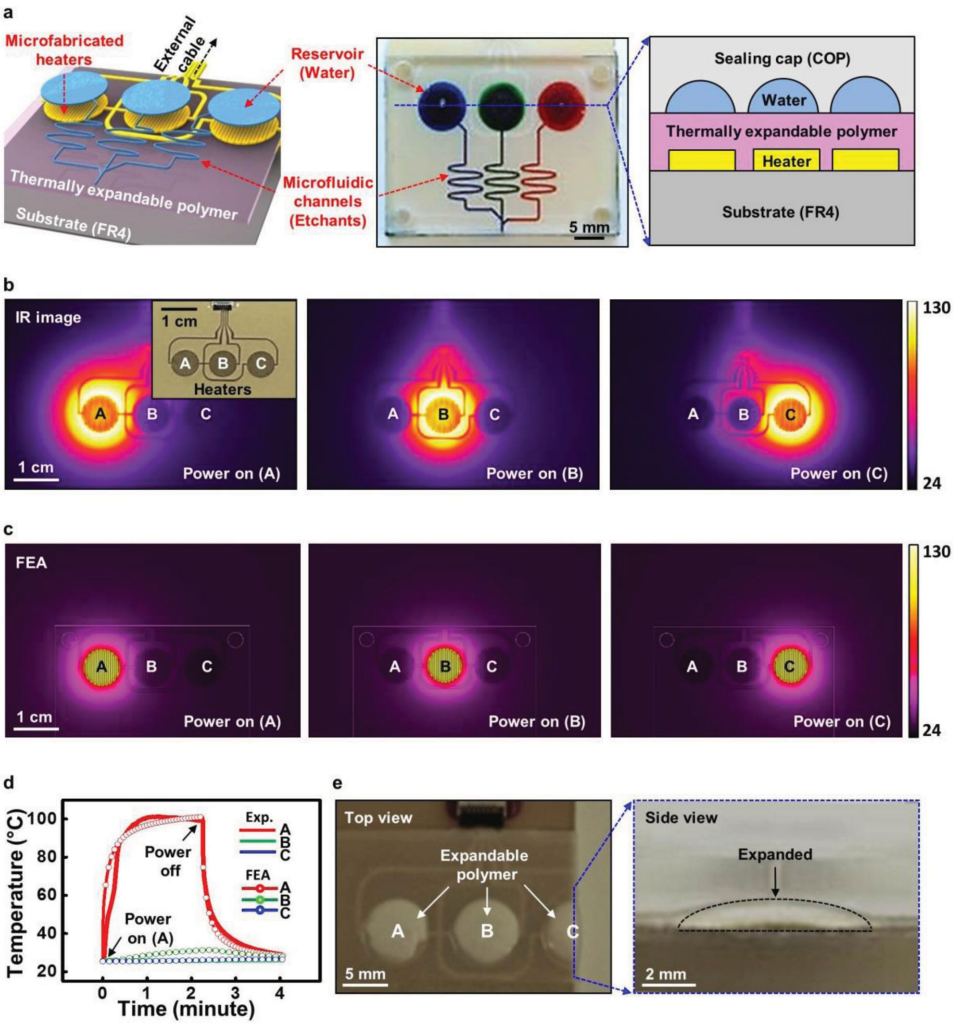

Figure 1. Layouts of a wireless microfluidic system for triggered transience and characterization of heater elements for actuating structures that serves as pumps. a) Schematic illustration (left), optical image (middle), and side view illustration (right) of the device, which consists of three independent microfluidic channels of COP, a layer of thermally expandable polymer and microfabricated heaters made of Au (300 nm) on a FR4 substrate. Water with red, green, and blue dye in each reservoir and microfluidic channel facilitates visualization. b) Infrared (IR) images of sequential powering of the heater elements (marked A, B, C). The inset shows a magnified optical image of the heaters. c) Corresponding results from FEA of the distributions of temperature. d) Experimental and computational (FEA) results of average temperatures of the heaters (marked A, B, C in Figure 1b and c). The temperature of the activated heater (marked A) reaches ≈100 °C while the others (marked B, C) remain at room temperature. e) Top and side view optical images of the thermally expandable polymer after full activation.

channels on a supporting substrate. The microfluidic system involves separate reservoirs and channels to eliminate the possibility for cross contamination. Three separate heater elements consist of serpentine traces of gold (300-nm thick) formed on top of an FR4 substrate, chosen for its use in conventional microelectronics and its low thermal conductivity (0.4 W m^{-1} K) with corresponding ability to reach high temperatures with minimum input power. The reservoirs and microfluidic channels consist of mechanically micromachined features of relief in a sealing cap made of a material (cyclic olefin polymer (COP)) that has low water vapor permeability (0.023 g mm m^{-2} d).[5] Images of these two separately prepared components appear in Figure S1, Supporting Information. Bonding this cap onto a layer of thermally expandable polymer (270-μm thick, Expancel 031 DU 40, AkzoNobel) spin cast on the FR4 substrate completes the fabrication. This polymer undergoes a rapid, abrupt, and irreversible change in volume at ≈80 °C. Details associated with the materials and fabrication procedures appear in the Experimental Section.

The wireless control system exploits serial communication with an infrared light-emitting diode (IR-LED, TSTS7100 IR emitter, wavelength: 950 nm, radiant intensity: 50 mW Sr^{-1}, Vishay Semiconductor) for the transmitter and an IR detector for the receiver, to allow independent control of each heater element in the microfluidic device. Experimental results summarized in Figure 1b illustrate sequential, wireless activation through thermal maps collected with an IR camera (FLIR SC650, Wilsonville, OR). Power delivered by a battery to the heaters (≈286 mW for each) induces Joule heating with peak temperatures of ≈100 °C within ≈20 s after wireless triggered

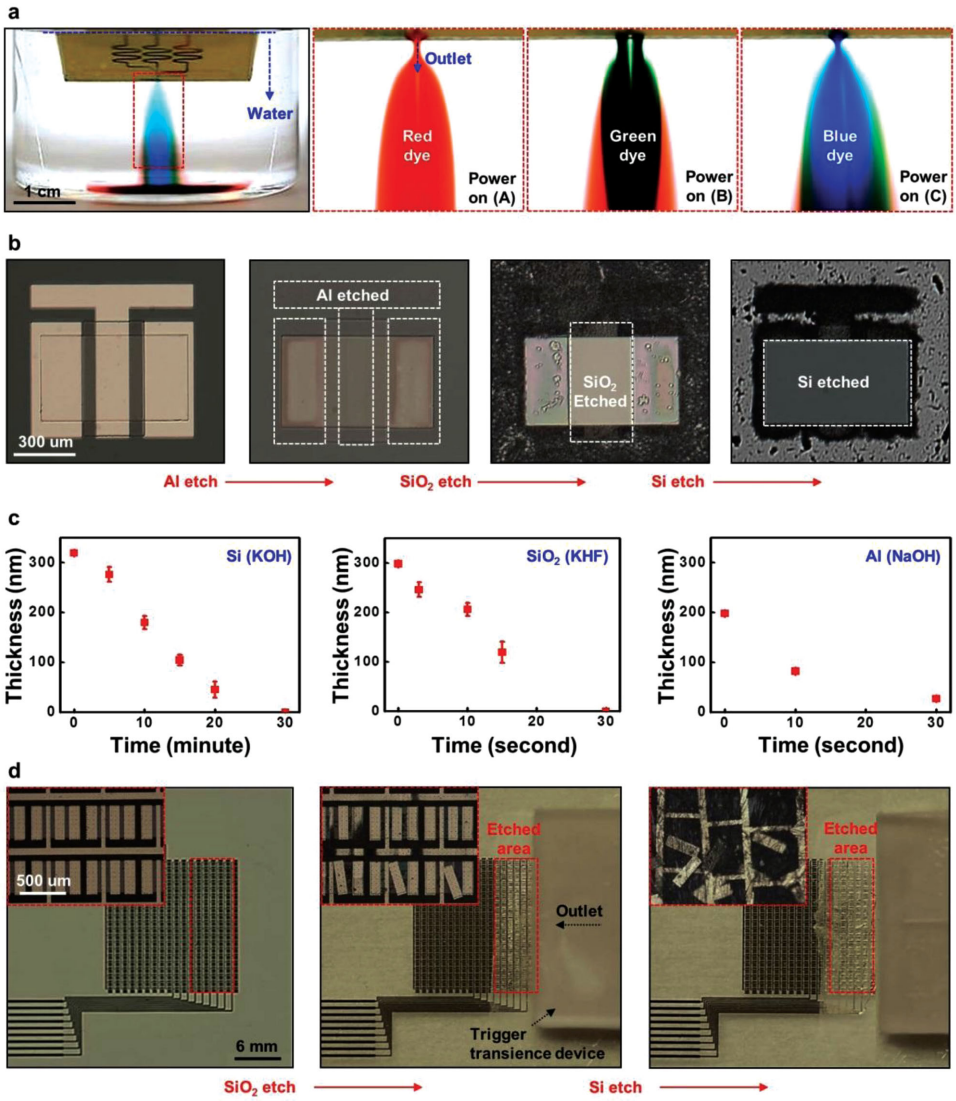

Figure 2. Illustrations of the operation of a wireless, microfluidic device for triggered transience. a) Optical images of the triggered release of water with red, green, and blue dye, sequentially with a time interval of ≈20 s. b) Sequence of optical microscope images after dissolution of Si, SiO_2, and Al by triggered release of corresponding etchants formed by mixing water with powders of KOH, KHF, and NaOH, respectively. c) Changes in thickness as a function of time for the dissolution of Si (left), SiO_2 (middle), and Al (right) in etchants formed with KOH, KHF, and NaOH at room temperature, respectively. d) Optical images of an array of MOSFETs before (left) and after the sequential triggered release of etchants formed with KHF (middle) and KOH (right). Insets shows microscope images at triggered area.

activation using an IR remote control unit (Movie S1, Supporting Information). These results agree with finite element analysis (FEA) of the coupled thermomechanical responses (Figure 1c). The temperature decreases rapidly from its peak value at the location of the operating heater to a value far below the activation temperature of the thermally expansive polymer in the surrounding regions, thereby allowing independent operation of the three reservoirs. The graph in Figure 1d shows experimental and computational FEA results of the average temperatures of the operating heater (marked A; ≈100 °C) and adjacent heaters (marked B and C; ≈room temperature) in Figure 1b (left). Activation of the thermally expandable polymer leads to its abrupt increase in volume (to ≈5 times of its original volume) within a minute, thus leading to complete filling of the reservoirs (Figure 1e). This process causes the ejection of ≈2.64 µL of water through the microfluidic channels, across the embedded chemical powders, and ultimately into overlap with the targeted electronics. The resulting etchants are capable of partially or completely dissolving layers of Si, SiO_2, Al, and other functional materials.

Figure 2a presents a demonstration of the triggered release process using water with red, green, and blue dyes. Activating each heater in a time sequence with intervals of ≈20 s via wireless control leads to ejection of the dyed water into a water bath (Movie S2, Supporting Information). Function in the manner envisioned here involves similar controlled release, but with different concentrated etchants selected to enable dissolution of the basic constituent components of conventional silicon

electronics and digital memory devices. Although removal of selected layers or materials can render a device nonfunctional, certain applications might call for complete destruction. For this demonstration, finely ground powders of potassium hydroxide (KOH, >85%, Fisher Scientific), potassium hydrogen fluoride (KHF, 99%, Sigma-Aldrich), and sodium hydroxide (NaOH, 99.99%, Sigma-Aldrich) yield, when mixed with water from the reservoirs, corrosive etchants for Si, SiO_2, and Al, respectively. We note that KOH and NaOH are hygroscopic, while KHF is not. Separation of the chemical powders (in the serpentine microfluidic channel structures) from the water (in the reservoirs) facilitates long-term storage without unwanted etching of the various components of the system. Conformal deposition of parylene (5-μm thick) on the inner walls of reservoirs and microfluidic channels further improves the chemical resistance and simultaneously prevents water in reservoirs from evaporating due to its excellent barrier properties and low water vapor permeability (0.08 g mm m^{-2} d).[6,7] Figure 2b presents a series of microscope images during the consecutive dissolutions of a test structure that consists of Al (200 nm), SiO_2 (300 nm), and Si (300 nm) formed by electron beam evaporation, plasma-enhanced chemical vapor deposition (PECVD, Plasmatherm) and reactive-ion etching (RIE, Plasmatherm) of the top layer silicon on a silicon-on-insulator (SOI, top silicon: 300 nm, SOITEC, France) wafer, respectively. When triggered, the water in the reservoirs mixes with the chemical powders as it passes through the serpentine microfluidic channels, thereby generating highly corrosive etchants at the outlet port. Values of pH measured at this location are 13.05, 4.28, and 12.10 for the cases of KOH, KHF, and NaOH powders, respectively. Figure 2c shows the thicknesses of various films evaluated by atomic force microscopy (AFM, Asylum Research MFP-3D, USA) at several stages during their dissolution at room temperature. Each material gradually disappears in a manner defined by the etching rates. Representative AFM images and thickness profiles appear in Figure S2, Supporting Information.

A practical demonstration example exploits an array of home-built metal-oxide-semiconductor field-effect transistors (MOSFETs) based on monocrystalline silicon nanomembranes (Si NMs), as in Figure 2d (left). The substrate supports 360 MOSFETs in an array, each with a mobility of ≈350 cm^2 $V^{-1}\cdot s$ and an on/off ratio $>10^4$, calculated from the representative transfer curves and current–voltage characteristics (Figure S3, Supporting Information). Details appear in the Experimental Section. Figure 2d (middle and right) provides a set of images collected after sequential, wireless triggered release of etchants based on KHF and KOH at room temperature. In ≈30 s after the trigger event, the etchants cause disintegration of the array into small fragments (Insets and Movie S3, Supporting Information).

An advantage of this type of device for triggered transience is that it naturally integrates with standard, commercially available semiconductor devices, including integrated circuits, memory devices, radios, micro-electro-mechanical systems components, sensors, and others. An example, shown in the images and schematic illustrations of **Figure 3**a,b uses a radio-frequency identification (RFID) device that consists of an unpackaged near field communication (NFC) chip (M24LR04E, ST Microelectronics) connected to a Cu inductive coil with an In/Ag solder paste (Figure 3a, inset). A layer of polydimethylsiloxane (Sylgard 184, Dow Corning) with a predefined hole (≈8 mm diameter) serves as a bonding interface that simultaneously directs the flow of etchant onto the NFC chip. Figure 3c,d illustrates the changes in key device characteristics, such as impedance and phase of the RFID device after the triggered release of etchant based on KHF. Flow onto the NFC chip yields significant and abrupt functional degradation within ≈3 s, with continued gradual degradation afterward. The observed degradation is attributed to the chemically destroyed NFC chip, coupled with the damaged interconnections between NFC chip and Cu coils. Microscope images in Figure 3e show the surface of the NFC chip before and after this process. Discoloration and roughening of the surface result from erosion induced by etching. Rinsing the eroded surface of NFC chip with acetone, methanol, and isopropanol removes residues for the purpose of facilitating further examination (Figure S4, Supporting Information).

3. Conclusion

The materials and design strategies introduced here provide platforms for electronics that are capable of irreversibly dissolving or disintegrating on demand. The same schemes are well suited to other kinds of sensors and microsystems technologies as well, where the goals might be to prevent unwanted proliferation of proprietary designs, as opposed to maintaining data security. For any such application, the ability to maintain sealed fluid compartments represents a key requirement. Although the systems described here are able to contain the liquids only for relatively short times (e.g., ≈7 d), advances in conventional microfluidics could extend the lifetime.

4. Experimental Section

Fabrication of Device for Triggered Transience: Photolithographic patterning of a film of Au (300 nm) formed by electron beam evaporation yielded heaters on an FR4 substrate (381-μm thick, ePlastics). A layer of thermally expandable polymer (270-μm thick; Expancel 031 DU 40, AkzoNobel) composed of a mixture of PDMS (Sylgard 184, Dow Corning) and Expancel at a ratio of 2:1 by weight, was spin cast and cured in a convection oven at 70 °C for 6 h. The thermally expandable microspheres consist of plastic shells that encapsulate a gas. Upon heating, the internal pressure of the gas increases and the shell softens. These combined effects cause a dramatic increase in the sizes of the microspheres, which is irreversible due to the thermoplastic nature of the deformation of the shells. Mechanical milling defined relief structures on a substrate of COP (2-mm thick, Zeon Chemicals). Depositing a conformal layer of 5-μm thick parylene formed a secondary seal to improve the chemical resistance and reduce permeability of water/vapor through the inner walls of reservoirs and microfluidic channels. Filling these features with finely ground chemical powders and bonding, the resulting substrate against the precured expandable layer using a double-sided adhesive film (ARclear, Adhesive Research) yielded sealed microfluidic channels. Distilled water (≈2.64 μL) was injected with a syringe into reservoirs through the predefined holes (≈0.45-mm diameter). Sealing the holes around the reservoirs and the outlets with Cu foil (300-nm thick) to prevent evaporation of water completed the fabrication.

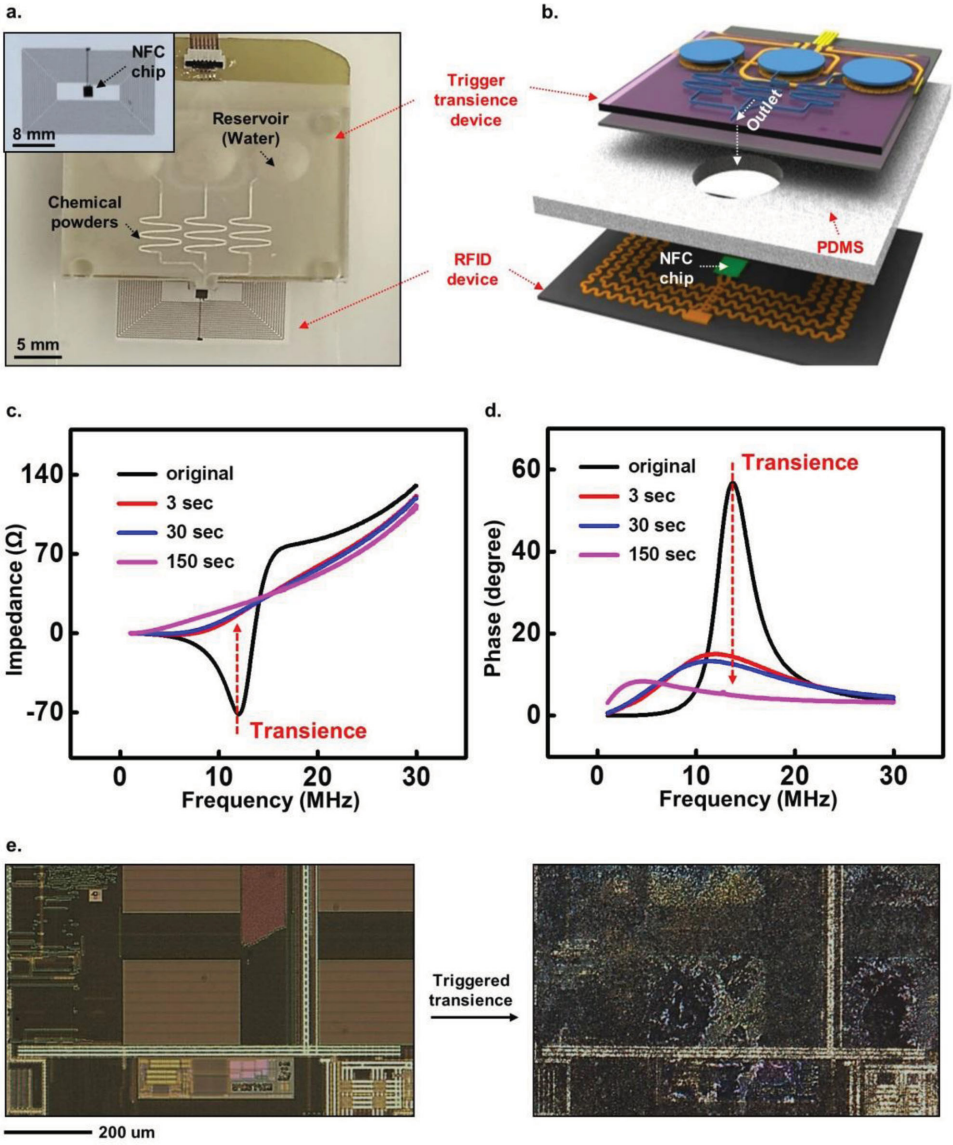

Figure 3. Wirelessly triggered transient RFID device. a) Optical image of the microfluidic system integrated with the RFID device. Inset shows a magnified view of an unpackaged NFC chip that provides essential function in the device. b) Exploded view schematic illustration of the full system. c,d) Measured changes in key device characterizations (e.g., impedance, phase) of the RFID device as a function of time after the triggered release of an etchant based on KHF. e) Microscope images of the commercial NFC chip before (left) and after (right) the triggered release of etchant based on KHF at room temperature.

Wireless Control System: A wireless transmitter (i.e., remote control) and a receiver provided communication through modulated IR signals. The transmitter included three buttons for control of the three individual heater elements. Pressing a button caused the microcontroller (Arduino Pro Mini 328, Arduino) in the transmitter to generate a corresponding control signal for emission of IR light from an LED, loaded onto a 38 kHz carrier frequency signal. The receiver consisted of a microcontroller (Attiny84, Atmel), an IR receiver (TSOP57438, Vishay Semiconductors), and transistors. The signal detected by the IR receiver activated the corresponding heater by turning on power supplied by a battery using an associated transistor as a switch.

Fabrication of an Array of Metal-Oxide-Semiconductor Field-Effect Transistors (MOSFETs): An array of MOSFETs using phosphorous doped Si NMs was prepared from silicon derived from an n-type SOI wafer. Phosphorous doping at 1 000 °C for 5 min defined highly doped areas for source and drain contacts. Removal of the buried oxide by wet etching with hydrofluoric acid released the top device silicon from the SOI wafer, and allowed transfer printing onto a film of polyimide (PI, 1 μm, Microchem) spin cast on a clean glass slide. Doped Si NMs were isolated by photolithography and reactive-ion etching (RIE, Plasmatherm) with sulfur hexafluoride (SF_6) gas. A thin layer of SiO_2 (100 nm) formed by plasma-enhanced chemical vapor deposition (PECVD, Plasmatherm) served as the gate dielectric. Photolithographic patterning and wet etching using buffered oxide etchant (BOE, Transene Company, USA) formed contact openings for source and drain electrodes. Depositing a layer of Au (150 nm) by electron beam evaporator to create the source, drain, and gate electrodes completed the process.

Fabrication of Radio Frequency Identification (RFID) Device: The process began with lamination of Cu foil (5 μm, Oak Mitsui Microthin series) onto a bilayer of PDMS (10 μm) and PI (2.4 μm) spin cast on a clean

glass slide. Photolithographic patterning and wet etching formed the inductive coil, and another layer of PI (2.4 μm) provided encapsulation. Contact openings for an interconnecting bridge were defined by using oxygen plasma etching and oxide remover (Flux, Worthington). A layer of electron beam evaporated Cu (2-μm thick) served as an interconnecting bridge. Photolithographic patterning and oxygen plasma removed unnecessary PI, leaving the PI only in the regions of the inductive coil. A thinned NFC chip (50-μm thick, M24LR04E, ST Microelectronics) was manually attached with an In/Ag solder paste (Ind. 290, Indium Corporation).

Supporting Information

Supporting Information is available from the Wiley Online Library or from the author.

Acknowledgements

C.H.L. and J.-W.J. contributed equally to this work. Financial support from National Science Foundation (NSF, DMR-12-42240) enabled the work. The experiments utilized the Frederick Seitz Materials Research Laboratory Central Facilities at the University of Illinois.

Received: October 13, 2014
Revised: November 23, 2014
Published online: December 23, 2014

[1] C. H. M. Shashank, S. Pandey, *Sensors IEEE*, IEEE, Baltimore **2013**.
[2] X. Gu, W. Lou, R. Song, Y. Zhao, L. Zhang, *Proc. of the 5th IEEE Int. Conf. on Nano/Micro Engineered and Mol. Syst.*, IEEE, Xiamen, China **2010**, 375.
[3] N. Banerjee, Y. Xie, H. Kim, C. H. Mastrangelo, *Sensors IEEE*, IEEE, Baltimore **2013**.
[4] S.-W. Hwang, H. Tao, D.-H. Kim, H. Cheng, J.-K. Song, E. Rill, M. A. Brenckle, B. Panilaitis, S. M. Won, Y.-S. Kim, Y. M. Song, K. J. Yu, A. Ameen, R. Li, Y. Su, M. Yang, D. L. Kaplan, M. R. Zakin, M. J. Slepian, Y. Huang, F. G. Omenetto, J. A. Rogers, *Science* **2012**, *337*, 1640.
[5] W. D. Niles, P. J. Coassin, *Assay Drug Dev. Technol.* **2008**, *6*, 577.
[6] T.-N. Chen, D.-S. Wuu, C.-C. Wu, C.-C. Chiang, Y.-P. Chen, R.-H. Horng, *Plasma Proc. Polym.* **2007**, *4*, 180.
[7] N. F. Sheppard, C. M. Feakes, *US 06973718*, **2005**.